Biochemistry and Biophysics Reports 6 (2016) 226–235

Contents lists available at ScienceDirect

Biochemistry and Biophysics Reports

journal homepage: www.elsevier.com/locate/bbrep

A method of water-soluble solid fraction saturation concentration evaluation in dry thalli of Antarctic lichenized fungi, *in vivo*

H. Harańczyk [a,*], P. Nowak [a], M. Lisowska [b], M. Florek-Wojciechowska [a], L.B. Lahuta [c], M.A. Olech [b]

[a] Institute of Physics, Jagiellonian University, Cracow, Poland
[b] Institute of Botany, Jagiellonian University, Cracow, Poland
[c] Department of Plant Physiology, Genetic and Biotechnology, University of Warmia and Mazury, Olsztyn, Poland

ARTICLE INFO

Article history:
Received 3 July 2015
Received in revised form
29 February 2016
Accepted 20 April 2016
Available online 22 April 2016

Keywords:
Lichenized fungi cetraria
Extremophilic organisms
Bound water
NMR

ABSTRACT

Background: At initial steps of rehydration from cryptobiosis of anhydrobiotic organisms or at rehydration of dry tissues the liquid ^{1}H NMR signal increased anomaly. The surplus in liquid signal may appear if some solid constituents dissolved, or if they were decomposed by enzymatic action.
Methods: Hydration kinetics, sorption isotherm, ^{1}H NMR spectra and high power relaxometry were applied to monitor gaseous phase rehydration of Antarctic lichen *Cetraria aculeata*. Tightly and loosely bound water signal were distinguished, and the upper hydration limit for dissolution of water soluble solid fraction was not observed. A simple theoretical model was proposed.
Results: The hydration courses showed a very tightly bound water fraction, a tightly bound water, and a loosely bound water fraction. Sigmoidal in form sorption isotherm was fitted well by multilayer sorption model. ^{1}H NMR showed one Gaussian signal component from solid matrix of thallus and one or two Lorentzian line components from tightly bound, and from loosely bound water. The hydration dependency of liquid signal was fitted by rational function.
Conclusions: Although in dehydrated *C.aculeata* the level of carbohydrates and polyols was low, the lichenase action during rehydration process increased it; the averaged saturation concentration $c_s = (57.3 \pm 12.0)\%$, which resembled that for sucrose.
General significance: The proposed method of water soluble solid fraction saturation concentration, c_s, calculation from ^{1}H NMR data may be applied for other organisms experiencing extreme dehydration or for dry tissues. We recalculated the published elsewhere data for horse chestnut (*Aesculus hippocastanum*) bast [water-soluble solid fraction recognized as sucrose, $c_s = (74.5 \pm 5.1)\%$]; and for *Usnea antarctica*, where $c_s = 0.81 \pm 0.04$.

1. Introduction

At initial steps of a very mild rehydration of some dry biological systems the liquid component of ^{1}H NMR signal does not increase proportionally with the increasing hydration level. Usually the observed dependency is well fitted using the rational function, *e.g.* in cellular organelles such as freeze-dried photosynthetic membranes [1,2]; in plant tissues like horse chestnut bast [3]; at the initial phases of seed imbibition [4], as well as in whole living organisms, *e.g.* in thalli of several species of lichenized fungi [5–9].

In extremely dry biological systems the carbohydrates and polyols remain completely/partially solidified (actual water concentration is far below their saturation hydration concentration point) and gradually dissolve with the increasing hydration level.

Carbohydrates and/or polyols play a critical role either for freezing resistivity [10] or in acute desiccation shock resistivity for numerous living organisms. For example, before dehydration to cryptobiosis *Polypedilum vanderplanki* larvae [11–12] accumulate large quantities of trehalose [13–16]. The major carbohydrate constituents of seed are starch (up to 80% dry mass of seed) and cellulose. In developing seed enzyme action decomposes starch to simple sugars, which remain in aqueous medium [4, 17–19]. The accumulation of monosaccharides and polyols in lichen mycobiont is an adaptive feature for dealing with the complete dehydration [20,21]. Ribitol level modifies the photosynthetic activity in some green algal foliose lichens [22].

^{1}H NMR relaxometry was applied to the analysis of extremely

* Correspondence to: Institute of Pysics, Jagiellonian University, ul. Łojasiewicza 11, 30-348 Cracow, Poland.
E-mail address: hubert.haranczyk@uj.edu.pl (H. Harańczyk).

http://dx.doi.org/10.1016/j.bbrep.2016.04.010

dry biological systems with a limited amount of water-soluble solid fraction. In horse chestnut bast it allowed to identify the water-soluble solid fraction as sucrose [3]. With the increased hydration level, as far as water-soluble solid fraction dissolves, the hydration dependency of total liquid ^{1}H NMR signal expressed in units of solid, *L/S*, is described by rational function, whereas for higher hydration levels at which the whole water-soluble solid fraction is completely dissolved the *L/S* hydration dependency becomes linear [3]. The presence of a threshold hydration level allows one to calculate the saturation concentration of water-soluble solid fraction, which may be used to identification of such a fraction.

In this report we propose a method for evaluation of the water-soluble solid fraction saturation concentration in case of a high amount of water-soluble solid fraction if the threshold hydration level is not detected, and if in the investigated biological system the signal coming from tightly bound water, L_1, and from loosely bound water signal, L_2, may be distinguished. A simple ^{1}H NMR experiment should be combined with sorption analysis for the investigated system.

As a model system we used a fruticose lichen *Cetraria aculeata* (Schreb.) Fr. thalli collected from sites in maritime Antarctica. Beside proton NMR spectra and relaxometry we recorded sorption kinetics, and sorption isotherms. The measurements were performed *in vivo*.

2. Theory

Harańczyk, Węglarz and Sojka [3] proposed that if the sample is hydrated by the mass, Δm, of water and if the water soluble solid fraction is present in the system, the amplitude of FID for liquid/mobile signal component may be expressed as a sum of three terms:

$$L = L_0 + \alpha_{H_2O}\rho_{H_2O}\Delta m + \alpha_{cd}\rho_c m_{cd} \quad (1a)$$

where L_0 (if such a fraction is detected) is the signal of water'sealed' in pores of dry solid matrix [1,2,23], the second term is proportional to the mass of water added, and the last one comes from water soluble solid fraction already dissolved. The amplitude of FID for solid signal component is then given by:

$$S = S_0 - \alpha_{cu}\rho_c m_{cd}, \quad (1b)$$

and:

$$S_0 = \alpha_s\rho_s m_0, \quad (1c)$$

where α_{H_2O}, α_{cd}, α_{cu} are the proportionality coefficients describing the effective contribution of a given proton pool to the total signal for water, and for water-soluble solid fraction in liquid and in solid phase, respectively (see Fig. 1). The values of coefficients α may be decreased *e.g.* by the presence of paramagnetic ions in the solution or on the surfaces of the solid matrix. If electron paramagnetism is absent in the investigated system $\alpha_i = 1$ [24]. However, in some biological systems solid NMR signal may be decreased by the presence of endogeneous electron paramagnetic ions, *e.g.* manganese [25]. The ρ_{H_2O} and ρ_c are proton densities of water and of water-soluble solid fraction, respectively, whereas m_{cd} is the mass of dissolved water-soluble solid fraction.

Knowing that the saturation concentration c_s of the water-soluble fraction is given by:

$$c_s = \frac{m_{cd}}{\Delta m + m_{cd}}. \quad (2)$$

The dissolved portion of water-soluble solid fraction, m_{cd}, may be obtained from:

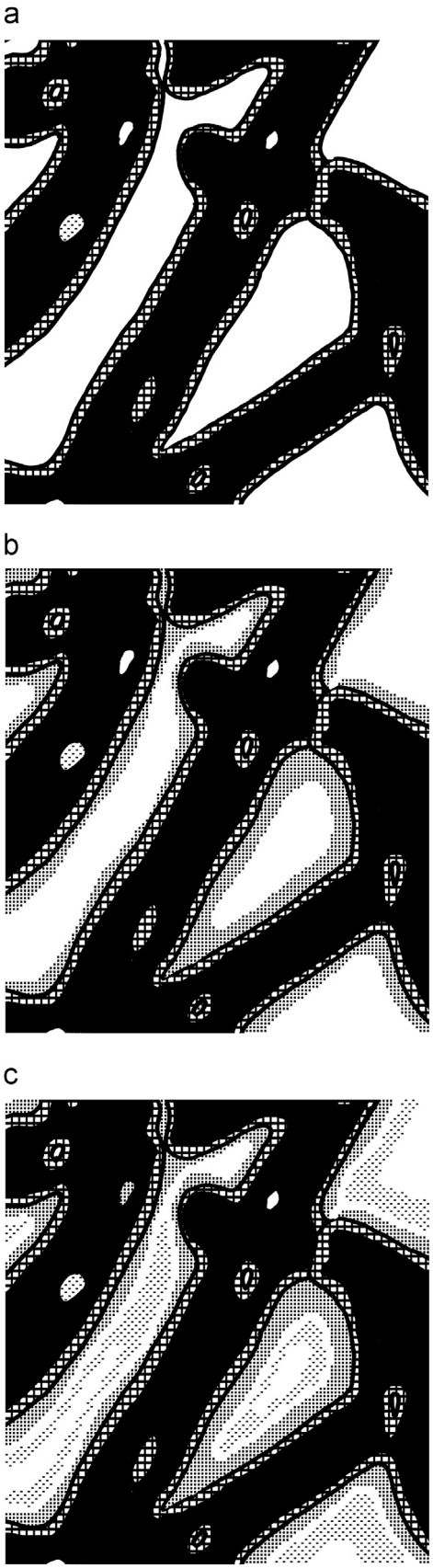

Fig. 1. Proton subsystems distinguished at rehydration of *C. aculeata* in dry thalli (a), at low hydration level (b), and in wet thalli (c): solid thallus, S_0, (black space); air (white space); undissolved water soluble solid fraction (rectangular grid); immobilized liquid fraction consisted of water soluble solid fraction dissolved to saturation concentration, c_s (dots), mobile liquid fraction consisted of water soluble solid fraction dissolved to c_s, and mobile water sealed in pores of dry solid (L_0) (fine dots).

$$m_{cd} = \frac{c_s}{1 - c_s}\Delta m. \tag{3}$$

In microheterogeneous systems bound water tend to orient depending on its mobility, and even tends to organize in some well defined layers [26]. If tightly bound water signal, L_1, may be distinguished from loosely bound water fraction L_2, the liquid signal component may be written as:

$$L = L_0 + L_1 + L_2 \tag{4}$$

and:

$$L_i = \left(\alpha^i_{H_2O}\rho_{H_2O} + \alpha_{cd}\rho_c\frac{c_s}{1 - c_s}\right)\Delta m_i, \tag{5}$$

where denumerator $i=1$, 2, and $\Delta m_2 = \Delta m - \Delta m_1$.

If the loosely bound (mobile) water pool filling the pores of the solid matrix is absent in the dry system, *i.e.* $L_0=0$, and if the proportionality coefficients for mobile and for immobilized water are equal, $\alpha^1_{H_2O} = \alpha^2_{H_2O}$, and also for water soluble solid fraction is $\alpha_{cd} = \alpha_{cu}$, so, the L_1 to L ratio may be written as:

$$\frac{L_1}{L} = \frac{m_1}{m_1 + \left(1 + \gamma\frac{c_s}{1-c_s}\right)\cdot\Delta m_2}, \tag{6}$$

where m_1 is the mass of water saturating tightly bound water pool and the coefficient γ describes the water-soluble solid fraction proton density to water proton density ratio:

$$\gamma = \frac{\rho_c}{\rho_{H_2O}}. \tag{7}$$

In the majority of living organisms which survive extreme dehydration the water-soluble solid fraction consists of sugars and/or polyols [5,11–14,20]. Table 1 presents the saturation concentrations, and γ symbols for carbohydrates and polyols frequently occurring in biological systems. We used them to calculate the average values of γ. The coefficient γ does not vary much between biological carbohydrates with the averaged value equal $\gamma = 0.59 \pm 0.01$. For polyols this value is quite similar and equals $\gamma = 0.67 \pm 0.06$. If the type of water-soluble solid fraction is not known, the mean value averaged over sugars and polyols is equal $\gamma = 0.63 \pm 0.08$.

The solid signal component, S_0, may be expressed as:

$$S_0 = \alpha_s\rho_s m_s, \tag{8}$$

where α_s is the responsible proportionality coefficient for the solid matrix of the lichen thallus, ρ_s is the averaged proton density for the solid matrix of the thallus, and m_s is the mass of the solid matrix of the thallus which in the absence of 'sealed' water fraction equals the dry mass of the sample, m_0. If water-soluble solid fraction is present, we get for the solid signal, S:

$$S = \alpha_s\rho_s m_0 - \alpha_{cu}\rho_c m_{cd}. \tag{9}$$

Thus, the total signal from liquid component may be expressed in units of solid component, L/S, [from (Eqs. (5) and 9)] as:

$$L/S(\Delta m/m_0) = \frac{\left(k + \frac{\alpha_{cd}}{\alpha_s}\gamma\frac{c_s}{1-c_s}\right)\Delta m/m_0}{1 - \frac{\alpha_{cu}}{\alpha_s}\frac{\rho_c}{\rho_s}\frac{c_s}{1-c_s}\cdot\Delta m/m_0}. \tag{10}$$

Assuming that the decrease of the NMR signal for dissolved water-soluble solid fraction is comparable to this for water we get $\frac{\alpha_{cd}}{\alpha_s} \approx k$, and if the proportionality coefficient for the undissolved water-soluble the solid fraction is similar to the rest of the solid matrix of thallus, $\frac{\alpha_{cu}}{\alpha_s} \approx 1$, we get:

$$L/S(\Delta m/m_0) = k\cdot\frac{\left(1 + \gamma\frac{c_s}{1-c_s}\right)\Delta m/m_0}{1 - \frac{\gamma}{\delta}\frac{c_s}{1-c_s}\cdot\Delta m/m_0} \tag{11}$$

where:

$$\delta = \frac{\rho_s}{\rho_{H_2O}}, \tag{12a}$$

and k is a slope of the L/S hydration dependence measured in case of the absence of water-soluble solid fraction expressed as:

$$k = \frac{\alpha_L\rho_L}{\alpha_S\rho_S}. \tag{12b}$$

Table 1
The saturation concentrations, c_s [27–32], proton densities and relative proton densities of carbohydrate and of the polyol fractions detected in photobiont and in mycobiont of Antarctic *Cetraria aculeata* thalli samples. For the carbohydrates the weighted average value of $\gamma = 0.59 \pm 0.01$, whereas for polyols it equals $\gamma = 0.67 \pm 0.06$.

Sugar	c_s	ρ_c	$\gamma = \frac{\rho_c}{\rho_{H_2O}}$	$\mathbf{10^{-3}\cdot\%}$
Fructose $C_6H_{12}O_6$	0.44	0.067	0.601	0.203± 0.004
Glucose $C_6H_{12}O_6$	0.54	0.067	0.601	0.085± 0.004
Sucrose $C_{12}H_{22}O_{11}$	0.68	0.064	0.580	1.23 ±0.05
Trehalose $C_{12}H_{22}O_{11}$	0.41	0.064	0.580	0.153 ±0.003
Polyol	c_s	ρ_c	$\gamma = \frac{\rho_c}{\rho_{H_2O}}$	$\mathbf{10^{-3}\cdot\%}$
Arabitol $C_5H_{12}O_5$	0.40	0.079	0.711	16.50±0.74
Myo-inositol $C_6H_{12}O_6$	0.13	0.067	0.601	0.82 ±0.03
Mannitol $C_6H_{14}O_6$	0.18	0.077	0.693	2.39 ±0.08

3. Materials and methods

Cetraria aculeata (Schreb.) Fr thalli were collected on Penguin Island (South Shetlands Islands), Oceanic Antarctica (62°13′S, 58°25′W), in 2009 at the altitude 110 m above sea level. Air-dry thalli were stored in herbarium at relative humidity $h \approx 40\%$ and at room temperature with the hydration level, $\Delta m/m_0 = 0.088 \pm 0.011$, where m_0 is the dry mass of the sample, and Δm is mass of water taken up. Vitality tests performed using methylene blue staining showed that no less than 62% photobiont cells of thalli samples were alive before the measurements.

Polyol and sugar contents were measured using high resolution gas chromatography (HRGC) method. Dry lichen thalli were crushed in a mixed mill (MM 200, Retch, Germany) set at the vibrational frequency of 22 Hz for 2 min. Carbohydrates were extracted from 25 to 30 mg of pulverized thalli (in 1.5-ml tubes) with 800 µl of extraction mixture (methanol: chloroform: water, 12:5:3, v/v/v) containing 100 µg of D-*chiro*-inositol as an internal standard. The homogenate was shaken on Genie 2 vortex (Scientific Industries, USA) for 2 min, heated at 60 °C for 30 min and centrifuged at 20,000*g* for 20 min at 4 °C. Aliquots (400 µl) of clear methanol-water supernatant were desalted, evaporated to dryness. The dry residue was derivatized with a mixture of trimethylsilylimidazole: pyridine (1:1, v/v) as described previously [31]. The TMS-derivatives of carbohydrates were separated on a Zebron ZB-1 capillary column (Phenomenex, USA) in GC-2010 gas chromatograph (Shimadzu, Japan). The column was operated with an initial temperature 140 °C adjusted to 160 °C at 5 °C min^{-1}, then to 200 °C at 10 °C min^{-1}, and finally to 290 °C at 30 °C min^{-1} (with total resolution time 11 min). The injection port operated in the split mode (10:1) at 325 °C, and the flame ionization detector was maintained at 350 °C. Helium was used as a carrier gas (with linear velocity 40 cm s^{-1}).

Soluble carbohydrates were quantified as described previously [33]. Standard of D-*chiro*-inositol (internal standard) was obtained from Industrial Research Ltd (New Zealand) and other

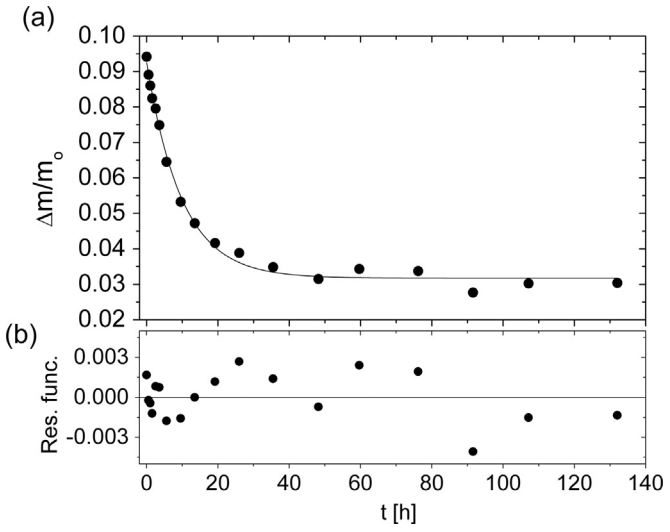

Fig. 2. (a) The dehydration of air dry *Cetraria aculeata* (Schreb.) Fr. thalli to gaseous phase at the relative humidity $h=0\%$, recorded as relative mass increase expressed in units of dry mass $\Delta m/m_0$. (b) The residual function calculated as the difference between the fitted and recorded values of the relative mass increase; the reduced value of $\chi^2=2.48$.

carbohydrates were purchased from Sigma-Aldrich. The results of analyses are the means of three independent replicates ± SE. Their values averaged for mycobiont and for photobiont are presented in Table 1.

Before the hydration courses thalli were incubated for 130 h over silica gel ($h=0\%$), dehydrating to the hydration level $\Delta m/m_0 = 0.031 \pm 0.003$. The dehydration process was well fitted by a single exponential function with the dehydration time $t_D = (14.11 \pm 0.65)$ h (See Fig. 2).

The hydration time-courses were performed from the gaseous phase with controlled humidity, at room temperature (t=22 °C), over the surface of H_3PO_4 ($h=9\%$), over the surface of saturated solutions of CH_3COOK ($h=23\%$), $CaCl_2$ ($h=32\%$), K_2CO_3 ($h=44\%$), $Na_2Cr_2O_7$ ($h=52\%$), NH_4NO_3 ($h=63\%$), $Na_2S_2O_3$ ($h=76\%$), K_2CrO_3 ($h=88\%$), Na_2SO_4 ($h=93\%$), K_2SO_4 ($h=97\%$), and over the water surface ($h=100\%$). Hydration kinetics courses were performed on one given sample per each value of relative humidity. After completing of the hydration courses, the dry mass of the thallus was determined after heating at 70 °C for 72 h. Higher temperatures were not used as they may cause decomposition of some organic constituents of the thallus [34].

The air-dry thalli designed for the NMR measurements were chopped, placed in NMR tubes, and incubated over silica gel, then the hydration procedure was performed. The NMR measurements were performed on fourteen samples. The measurements of a drier sample covered a part of hydration range for the next more wet sample, whereas the hydration level was calculated as $\Delta m/m_0$.

^{1}H NMR spectra were collected on Bruker Avance III spectrometer (Bruker Biospin), operating at the resonance frequency 300 MHz (at $B_0=7$ T), with the transmitter power equal to 400 W. The pulse length was $\pi/2=1.5$ μs, bandwidths 300 kHz, and repetition time was 2 s.

^{1}H NMR free induction decays (FIDs) were recorded using WNS HB-65 high power relaxometer (Waterloo NMR Spectrometers, St. Agatha, Ontario, Canada). The resonance frequency was 30 MHz (at $B_0=0.7$ T); the transmitter power was 400 W; and the pulse length $\pi/2=1.5$ μs. In every FID 120 data points were collected, which were ordered in three equal groups with the different time-spacings equal to 0.4 μs, 2.5 μs, and 10 μs. The quadrature detection was applied, and the value of FID was a square root from the sum of squares of the phased and the dephased channel signals, Re^2+Im^2. FIDs were acquired using Compuscope 2000 card of an IBM clone controlling the spectrometer and averaged over 2000 accumulations.

The data obtained were analyzed using the FID analyzing procedure of a two-dimensional (in time domain) NMR signal-analyzing software CracSpin written at the Jagiellonian University, Cracow [35], or by commercially available software Origin 7.0.

4. Results

4.1. Hydration kinetics

The hydration courses for *Cetraria aculeata* were performed from the gaseous phase, and were fitted well by single exponential function for the relative humilities, h, controlled between 9% and 52% (see Fig. 3):

$$\Delta m/m_0 = A_0^h + A_1^h \cdot \left[1 - \exp(-t/t_1^h)\right], \tag{13a}$$

where $\Delta m/m_0$ is the relative mass increase expressed in units of dry mass, m_0, A_1^h is the saturation level for the fast component solely observed at a given relative humidity range, and A_0^h is the hydration level at $h=0\%$ (very tightly bound water fraction).

As relative humidity exceeded 63% the slow hydration component appeared, and the hydration courses were fitted well by the two exponential function (Fig. 3):

$$\Delta m/m_0 = A_0^h + A_1^h \cdot \left[1 - \exp(-t/t_1^h)\right] + A_2^h \cdot \left[1 - \exp(-t/t_2^h)\right], \tag{13b}$$

where A_0^h is the saturation level of very tightly bound water fraction (at $h=0\%$), A_1^h and A_2^h are the saturation hydration levels for the fast and for the slow component, and t_1^h and t_2^h are hydration times for fast and slow component (tightly and loosely bound water fraction), respectively.

The averaged (over the all hydration courses) value of $A_0^h = 0.04 \pm 0.02$. It is a very tightly bound fraction of water, which is not removed by dehydration over silica gel surface. Its relative mass is close to that obtained for other species of Antarctic lichens, *e.g.* for fruticose *Usnea antarctica* Du Rietz $A_0^h = 0.040 \pm 0.011$, [6], and for foliose *Umbilicaria aprina* Nyl. $A_0^h = 0.054 \pm 0.011$ [7].

The amplitude of the tightly bound water fraction equals to

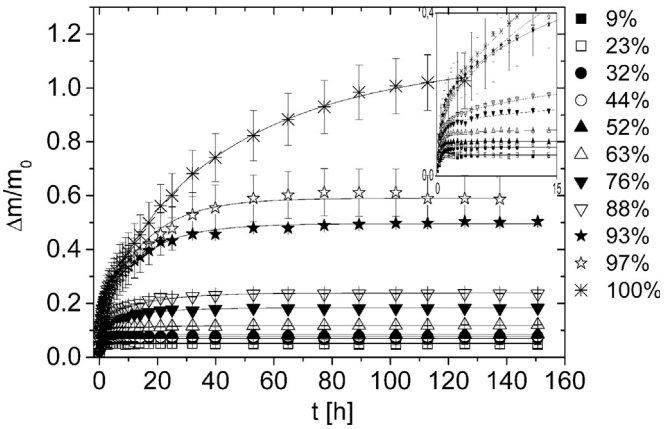

Fig. 3. The rehydration of the lichen *Cetraria aculeata* (Schreb.) Fr. from gaseous phase at different values of relative humidity h, recorded as relative mass increase expressed in units of dry mass $\Delta m/m_0$. Targets humidity: $h=9\%$ – closed squares, $h=23\%$ – open squares, $h=32\%$ – closed circles, $h=44\%$ – open circles, $h=52\%$ – closed triangles, $h=63\%$ – open triangles, $h=76\%$ – closed reversed triangles, $h=88\%$ – open reversed triangles, $h=97\%$ – close starlets, $h=100\%$ – asterisks. The error bars are within the plot symbols.

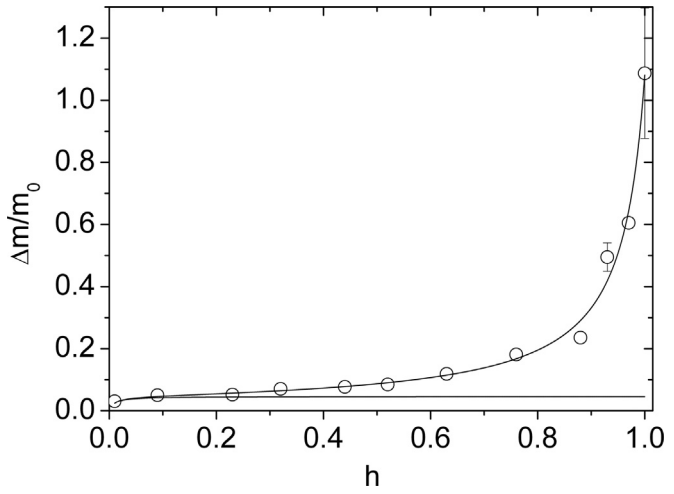

Fig. 4. The sorption isotherm for *Cetraria aculeata* (Schreb.) Fr. The values of h represent the relative humidity, and the values of relative mass increase, $\Delta m/m_0$, are taken as the saturation values, C^h, from hydration kinetics (open circles = experimental data). Fitted Dent multilayer sorption model (Eq. (2)) (solid line = fitted Dent model), and 'primary' water binding sites monolayer coverage for Dent isotherm equal $\frac{\Delta m}{m_0} = \frac{\Delta M}{m_0}\cdot\frac{b_1 h}{1+(b_1-b)h}$ [36] (dotted line = fitted 'primary' water binding sites population).

$A_1^h = 0.037 \pm 0.005$, with the hydration time $t_1^h = (0.43 \pm 0.10)$ h, whereas the loosely bound water fraction appearing for the courses performed from the values of relative humidity higher than 63% is characterized by the hydration time equal to $t_2^h = (14.2 \pm 6.2)$ h. The saturation level of the loosely bound water component, A_2^h, increases gradually with increased humidity.

Loosely and tightly bound fractions may be distinguished by their proximity to the surface of solid matrix and thus by their mobility.

The total saturation hydration level, $C^h = A_0^h + A_1^h + A_2^h$, obtained at a given relative humidity, h, was taken for construction of sorption isotherm.

4.2. Sorption isotherm

For *Cetraria aculeata* thalli the sorption isotherm is sigmoidal in form (Fig. 4), which usually is well fitted by the multilayer sorption models distinguishing two types of water binding sites on the surfaces of the investigated system, namely, (i) 'primary' water binding sites (directly bound to the adsorbent surface); and (ii) 'secondary', usually weaker, water binding sites (to the previously bound water molecules, or to the weaker binding sites on a solid matrix surface). The most commonly applied ones are the classic BET model [36], and GAB (Dent) model [37]. BET model takes a fixed value of the ratio of binding sites covered by n water molecules expressed in units of binding sites covered by *n-1* water molecules $b = S_n/S_{n-1}|_{h=1} = 1$, which is to some extent an artificial assumption, whereas in Dent model this number may be varied between 0 and 1 (somehow simulating the clustering effect), and is equal $b = S_n/S_{n-1}|_{h=1}$. Sorption isotherm for both models is expressed by:

$$C^h(h) = \frac{\Delta M}{m_0}\frac{b_1 h}{(1-bh)\cdot(1+b_1 h - bh)} \tag{14}$$

where h is relative humidity expressed in absolute units, $\Delta M/m_0$ is the mass of water saturating primary binding sites, where S_i is the number of binding sites covered by i water molecules, and the contribution of empty primary binding sites, S_0, on the surface in units of sites with one water molecule, S_1, at $h=1$ is expressed by the reciprocal of b_1: $S_0/S_1|_{h=1} = 1/b_1$.

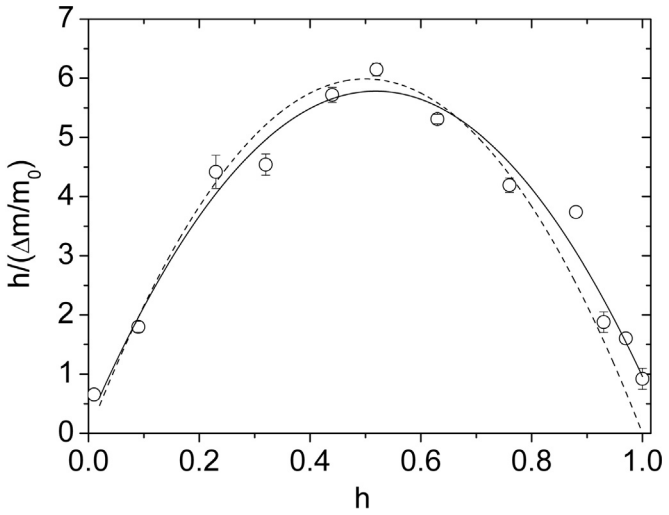

Fig. 5. Parabolic form of Dent and BET model (open circles – experimental data, solid line – fitted Dent model (Eq. (3)b), dotted line – fitted BET model (Eq. (3)a)).

To test the relevance of the model used the sorption isotherm is usually presented in parabolic form (see Fig. 5), which for BET model is expressed as:

$$\frac{h}{\Delta m/m_0} = A + Bh - (A+B)h^2, \tag{15a}$$

whereas for Dent model as:

$$\frac{h}{\Delta m/m_0} = A + Bh - Ch^2, \tag{15b}$$

where parameters $\frac{\Delta M}{m_0}$, b, b_1 are connected with A, B, C by the formulas:

$$b = \frac{\sqrt{B^2+4AC} - B}{2A} \tag{16a}$$

$$b_1 = \frac{B}{A} + 2b \tag{16b}$$

$$\frac{\Delta M}{m_0} = \frac{1}{Ab_1} \tag{16c}$$

For *Cetraria aculeata* thalli the sorption isotherm is much better described by Dent model, as the parameter equals $b = 0.958 \pm 0.003$. The sorption isotherm for other Antarctic lichens is also better fitted using Dent model, *e.g.* for *Leptogium puberulum* $b = 0.955$ [8], for *Umbilicaria aprina* $b = 0.941$ [7], and for *Usnea antarctica* $b = 0.913$ [6].

The mass of water saturating primary water binding sites is equal $\Delta M/m_0 = 0.046 \pm 0.003$, which is very close to the value obtained from hydration kinetics for very tightly bound water pool.

The proportion of unoccupied water binding sites at $h=1$ equals for *Cetraria aculeata* $1/b_1 = 0.925\%$. This result is comparable with values reported for other lichens, *e.g.* for *U. aprina*, $1/b_1 = 0.02\%$ [7], *Himantormia lugubris* $1/b_1 = 1.11\%$, and for *Caloplaca regalis* $1/b_1 = 1.93\%$ [5].

4.3. ^{1}H NMR spectra

Fig. 6 shows ^{1}H NMR spectra for *C. aculeata* thalli recorded at 300 MHz at two different hydration levels. For *C. aculeata* at the lower hydration level ($\Delta m/m_0 = 0.112$) the spectrum was the superposition of the broad component coming from the solid matrix

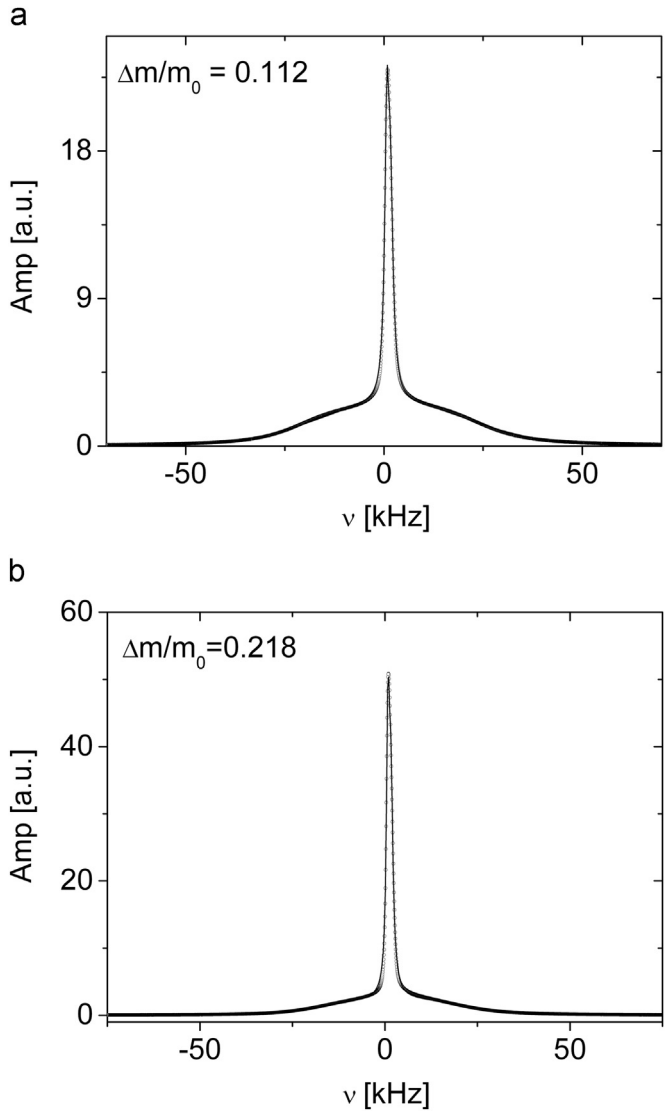

Fig. 6. ^{1}H NMR spectra for *Cetraria aculeata* (Schreb.) Fr. thalli recorded at 300 MHz; the pulse length $\pi/2=1.5$ μs. The relative mass increase was (a) $\Delta m/m_0=0.112$, and (b) $\Delta m/m_0=0.218$.

of the lichen thallus, which may be successfully fitted by Gaussian function, and two narrow components coming from water bound in thallus, both fitted by Lorentzian functions (Eq. (17)):

$$A(\nu)=\frac{A_S}{\Delta\nu_G\cdot\sqrt{\ln\ 4\cdot\pi/2}}\exp\left[-2\ \ln\ 4\cdot\left(\frac{(\nu-\nu_G)}{\Delta\nu_G}\right)^2\right]+\frac{2A_{L_1}}{\pi}\left[\frac{\Delta\nu_{L_1}}{4\cdot\left(\nu-\nu_{L_1}\right)^2+\Delta\nu_{L_1}^2}\right]+\cdots\cdots+\frac{2A_{L_2}}{\pi}\left[\frac{\Delta\nu_{L_2}}{4\cdot\left(\nu-\nu_{L_2}\right)^2+\Delta\nu_{L_2}^2}\right], \quad (17)$$

where $\Delta\nu_G$, $\Delta\nu_{L_1}$, and $\Delta\nu_{L_2}$ are the half-widths of the NMR line,; ν_G, ν_{L_1}, and ν_{L_2} are peak positions,; and finally A_S, A_{L_1}, and A_{L_2} are the amplitudes of the Gaussian and two Lorentzian peaks, respectively.

With the increased hydration level (at $\Delta m/m_0=0.218$) the tightly bound water fraction is no longer fitted, and the spectrum is fitted by the superposition of one Gaussian component, and only one Lorentzian component coming from loosely bound water fraction, according to:

$$A(\nu)=\frac{A_S}{\Delta\nu_G\cdot\sqrt{\ln\ 4\cdot\pi/2}}\exp\left[-2\ \ln\ 4\cdot\left(\frac{\nu-\nu_G}{\Delta\nu_G}\right)^2\right]+\frac{2A_L}{\pi}\left[\frac{\Delta\nu_{L_2}}{4\cdot\left(\nu-\nu_{L_2}\right)^2+\Delta\nu_{L_2}^2}\right], \quad (18)$$

The halfwidths of the solid line component in the Gaussian approximation decrease from $\Delta\nu_G=(46.4\pm0.2)$ kHz down to (43.4 ± 0.7) kHz, with the hydration level increased from $\Delta m/m_0=0.112$ up to 0.218. Tightly bound water (broader) line component is detected only for the sample at the lower hydration level, with $\Delta\nu_{L_1}=2.238$ kHz, whereas for the higher hydration level it is not detected by a fitting procedure. For the loosely bound water liquid component, the halfwidth is equal *ca.* $\Delta\nu_{L_2}=1.422$ kHz, which is close to the value $\gamma\cdot\Delta B_0$ of the line-widths broadened by the B_0 inhomogeneities. Table 2 sets up the parameters of the recorded spectra.

4.4. Proton free induction decays

Free induction decay for protons of the *Cetraria aculeata* thallus may be sufficiently well fitted by the superposition of one Gaussian component, with the amplitude *S*, coming from the solid matrix of the thallus; and one with the amplitude equal to L_1 or for higher hydration levels two, L_1 and L_2, exponential components coming from water tightly and loosely bound on the surfaces of the thallus, respectively [3,6,7]:

$$FID(t)=S\cdot\exp\left(-\left(\frac{t}{T_{2S}^*}\right)^2\right)+L_1\cdot\exp\left(-\frac{t}{T_{2L_1}^*}\right)+L_2\cdot\exp\left(-\frac{t}{T_{SL_2}^*}\right) \quad (19)$$

where T_{2S}^* is the proton relaxation time of the solid component taken for 1/e-value of the Gaussian solid signal, and $T_{2L_1}^*$ and $T_{2L_2}^*$ are the relaxation times of proton liquid fractions L_1 and L_2 respectively (Fig. 7).

However, a more precise analysis reveals the presence of a "beat pattern" [38,39] and in such a case the solid component of FID signal is better approximated by the Abragam function [40]:

$$S(t)=\exp\left[-\left(\frac{t}{T_{2S}^*}\right)^2\right]\frac{\sin\ at}{at}. \quad (20)$$

To estimate the error made by the Gaussian approximation, the moment expansion of the solid component of the FID signal was performed:

$$S(t)=S\left(1-\frac{M_2}{2!}t^2+\frac{M_4}{4!}t^4-\frac{M_6}{6!}t^6+\ldots\right), \quad (21)$$

where M_i is the *i*-th moment of the absorption line, and *t* is the time starting from the final slope of /2 pulse.

Table 2
The parameters fitted to the ^{1}H NMR spectra for *Cetraria aculeata* thalli recorded at room temperature for two different hydration levels.

$\Delta m/m_0$	ν_G [Hz]	$\Delta\nu_G$ [kHz]	ν_{L_1}Z [Hz]	$\Delta\nu_{L_1}$Z [kHz]	ν_{L_2}Z [Hz]	$\Delta\nu_{L_2}$Z [kHz]	L/S^*	L/S (FID)
0.112	2450 ± 80	46.4 ± 0.2	1535 ± 23	2.24 ± 0⊡2	821 ± 7	1.27 ± 0.02	0.463	0.338
0.218	3680 ± 250	43.4 ± 0.7	–	–	1151 ± 2	1.57 ± 0.01	1.348	0.719

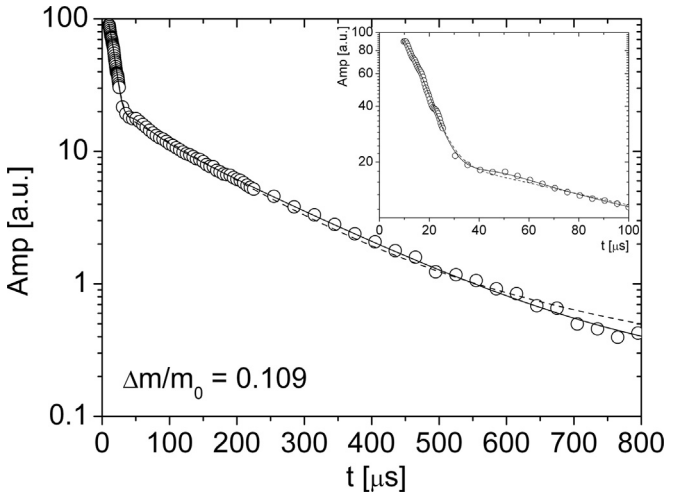

Fig. 7. The proton FID function recorded at 30 MHz for *Cetraria aculeata* (Schreb.) Fr. thalli hydrated to the relative mass increase $\Delta m/m_0=0.109$; the superposition of Gaussian and two exponents (Eq. (14)) is fitted (dotted line); if the superposition of Abragam function (Eq. (16)) and two exponentials (solid line)fits the characteristic "beat" pattern (better seen on the inset).

For Abragam function the moment expansion equals [40]:

$$S(t) = 1 - \left(\frac{2}{(T_{2S}^*)^2} + \frac{1}{3}a^2\right)\frac{t^2}{2!} + \left(\frac{12}{(T_{2S}^*)^4} + \frac{4a^2}{(T_{2S}^*)^2} + \frac{1}{5}a^4\right)\frac{t^4}{4!} - \left(\frac{120}{(T_{2S}^*)^6} + \frac{60a^2}{(T_{2S}^*)^4} + \frac{6a^4}{(T_{2S}^*)^2} + \frac{a^6}{7}\right)\frac{t^6}{6!} + \ldots \quad (22)$$

where for second, fourth, and for sixth moment we get, respectively:

$$M_2 = \frac{2}{(T_{2S}^*)^2} + \frac{1}{3}a^2 \quad (23a)$$

and:

$$M_4 = \frac{12}{(T_{2S}^*)^4} + \frac{4a^2}{(T_{2S}^*)^2} + \frac{1}{5}a^2 \quad (23b)$$

and:

$$M_6 = \frac{120}{(T_{2S}^*)^6} + \frac{60a^2}{(T_{2S}^*)^4} + \frac{6a^4}{(T_{2S}^*)^2} + \frac{a^6}{7}. \quad (23c)$$

Hence, for the Gaussian approximation of the solid signal ($a\rightarrow 0$) we get:

$$\frac{M_4}{M_2^2} = 3, \quad (24a)$$

and

$$\frac{M_6}{M_2^3} = 15. \quad (24b)$$

For the *Cetraria aculeata* thalli the moment expansion of the solid component of FID signal gives $M_2=3.9\cdot 10^9\ s^{-2}$, $M_4=4.0\cdot 10^{19}\ s^{-4}$, and $M_6=2.5\cdot 10^{29}\ s^{-6}$, with the magnitude S=106.9. The solid line was nearly Gaussian (with $\frac{M_4}{M_2^2}=2.46$), thus for the next routine measurements the solid line was approximated by a Gaussian function (Eq. (6)). In fact, the solid signal for lichen thalli is often nearly Gaussian in form [6–8].

Relaxation time for the solid component, $T_{2S}^*\approx 21$ μs, is close to the value obtained for other lichens, and different solid biological systems as lyophilized photosynthetic membranes [1,2], lyophilized model membranes from DGDG [23], or lyophilized DNA [41], which suggests similar distribution of local magnetic fields for limited number of chemical groups forming the biological system at a submolecular scale [42].

The observed water fractions are differentiated by their mobility and thus by their binding and/or proximity to the solid thallus surfaces, which means that intracellular water as well as extracellular water fractions usually contributes to both these water fractions. The $T_{2L_1}^*\approx 120$ μs of the L_1 component is characteristic for tightly bound water of lichen thalli as well as of many other biological systems [*e.g.* 5, and the references therein]. The L_2 signal with $T_{2L_2}^*\approx 560$ μs, shortened by B_0 inhomogeneities, comes from water loosely bound on the thallus surface and for the higher hydration level from free water fraction (Fig. 7).

The spin-spin relaxation times measured in FID experiment are shortened by B_0 inhomogeneities according to [43]:

$$\frac{1}{T_2^*} = \frac{1}{T_2} + \frac{\gamma\Delta B_0}{2} \quad (25)$$

where T_2 is the spin-spin relaxation time, γ is the gyromagnetic ratio, and ΔB_0 is a change of magnetic field B_0 within the sample. The solid and short exponential components are detected and not changed (as compared to CPMG echo train), but L_2 may be an average of several loosely bound water pools, eg. extra- and intramolecular loosely bound water fraction.

4.5. The hydration dependence of NMR signal

Fig. 8 shows the *a* parameter obtained from the Abragam function (Eq. (2)0) fitted to FIDs recorded for *Cetraria aculeata* thalli as a function of the hydration level. The parameter decreases slightly with the hydration level, which remains in correspondence with the change of the solid component halfwidth (a decrease from 32 kHz down to 25 kHz with hydration level increase from $\Delta m/m_0=0.04$ up to 0.2). For the higher hydration level the 'beat pattern' characteristic for Abragam function is no longer detected.

For the hydration level below $\Delta m/m_0=0.18$ a tightly bound water, L_1, and a loosely bound water component, L_2, are detected (Eq. (19)). For the tightly bound water component, the relaxation time $T_{2L_1}^*\approx 100$ μs, whereas for the loosely bound water component the effective relaxation time equals $T_{2L_2}^*\approx 100$ μs (see Fig. 9).

For *Cetraria aculeata* the relaxation time T_{2S}^* of the solid component (in a Gaussian approximation) does not change much with

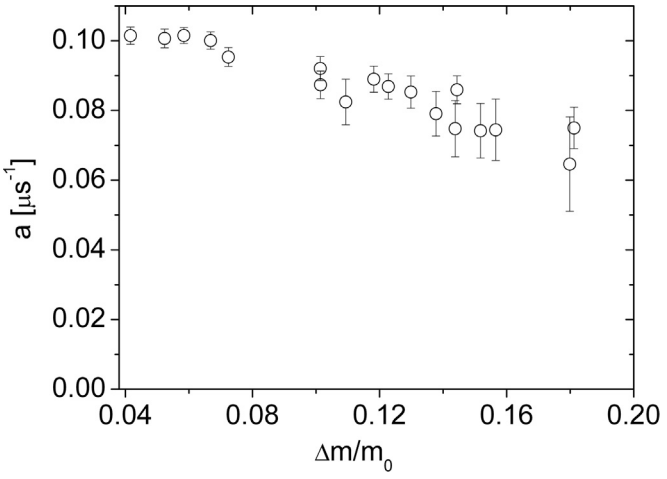

Fig. 8. The parameter *a* for Abragam function fitted to solid component signal (thallus solid matrix line widths) calculated for *Cetraria aculeata* (Schreb.) Fr. thalli as a function of hydration level recorded as relative mass increase expressed in units of dry mass $\Delta m/m_0$.

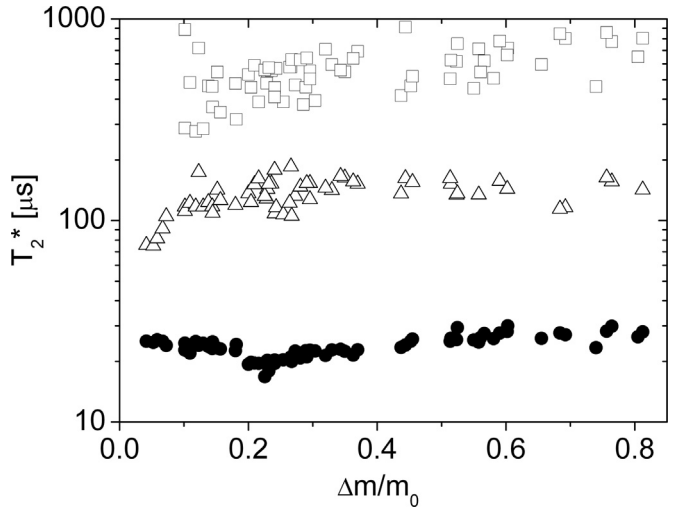

Fig. 9. The hydration dependence of proton FID relaxation times for *Cetraria aculeata* (Schreb.) Fr. Solid Gaussian, S, component – closed circles, tightly bound water, L_1, component – open triangles, and loosely bound water, L_2, fraction – open squares.

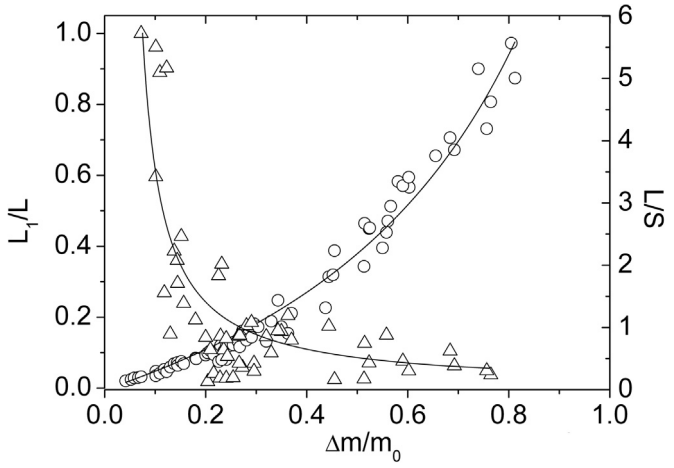

Fig. 11. The tightly bound water in units of total liquid signal, L_1/L, (open triangles) and the total liquid signal in units of solid, L/S, (open circles) hydration dependence for *Cetraria aculeata* (Schreb.) Fr. The solid lines were calculated from Eq. (6) and from Eq. (11), respectively.

the thallus hydration level (Fig. 9), which suggests that the structure and molecular dynamics of the thallus solid matrix are not much modified by the hydration process. Thus, we used a solid signal amplitude, *S*, as an unit to scale the amplitudes of liquid components.

Fig. 10 shows the hydration dependence of the tightly and of loosely bound water signal amplitude in units of solid amplitude, L_1/S and L_2/S, respectively. The hydration level is expressed as the relative mass increase in units of dry mass of the thallus, $\Delta m/m_0$. The tightly bound water signal, L_1/S, does not change within the measured hydration range, which suggests that it has already saturated for a lower hydration level. The hydration dependence of mobile (loosely bound) water signal, L_2/S, increases with the relative mass increase and is well fitted by a rational function.

That the rational function successfully models the dependence, suggests the application of Eq. (6) for L_1/L hydration dependence, and Eq. (11) for the L/S hydration dependence for the *Cetraria aculeata* thallus. The combined fit of Eq. (6) and Eq. (11) performed for $\gamma = 0.63 \pm 0.08$ is presented on Fig. 11. The lowest hydration level at which L_2 signal component is detected (and thus L_1/L becomes less than 1) is fitted as $\Delta M_1/m_0 = 0.075 \pm 0.006$ (see Fig. 10 for comparison). The saturation concentration of the water-soluble solid fraction is $c_p = 0.57 \pm 0.12$.

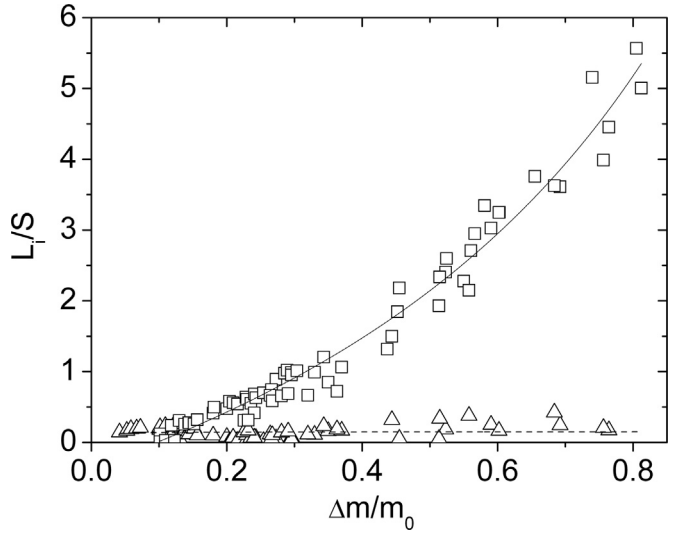

Fig. 10. Tightly bound water component, L_1/S, and loosely bound water component, L_2/S, hydration dependence for *Cetraria aculeata* (Schreb.) Fr. The solid line is a rational function fitted (See text).

5. Discussion

Although the model proposed by the Authors yields the averaged saturation concentration for water-soluble solid fraction as equal to $c_s = (57.3 \pm 12.0)\%$, which is close to the value for averaged carbohydrate and polyol saturation concentration calculated for *Cetraria aculeata* thallus $(65.7 \pm 8.3)\%$, the actual concentration of carbohydrates and polyols in the dry thallus is much too small to be responsible for the nonlinearity in L/S hydration dependence.

Thus, it can be suggested than other cellular compounds are responsible for *C. aculeata* thallus hydration. Lichen thalli are known to contain considerable amounts of water-soluble glucans: lichenin, a hot-water-soluble linear (1→3) (1→4)-β-glucan and isolichenin, a cold-water-soluble (1→3) (1→4)-α-glucan, both with different proportions of linkage groups in diverse taxa of lichens. Honegger and Haisch [44] revealed that in fully hydrated and desiccated thalli of *C. islandica,* both the cortical extracellular matrix and the outer wall layer of medullary hyphae shrink dramatically during drought stress, indicating that these are major sites of water storage. Moreover authors suggested that a mycobiont derived, hydrophilic wall surface layer prevents the thallus interior from becoming waterlogged at full hydration. Similar properties, such as solubility and rheological behaviour in the solution and gel states, indicate cereal *β*-glucans, occurring in grasses (among them also cereals), lower plants and fungi [45,46]. In seeds glucans play a role of storage material, which is degraded during seed germination [47]. Thus, it can be suggested that lichenin and isolichenin are also hydrolyzed in hydrated lichen thalli, according to the metabolic/physiological demand of cells. However, the content of glucans in *C. aculeata* was not analyzed in our study. Therefore we can only speculated that during thallus rehydration, causing the return of lichenized fungus from the cryptobiotic state, the additional pool of monosaccharides is supplied by the enzymatic action of endoglucanases. In such situation, our results could be a confirmation of the effect of the enzymatic action on lichen polysaccharides resulted in increase in monosaccharide concentration in lichen thallus returning from cryptobyosis state during rehydration. That could be a reason why L/S hydration dependence is well fitted by our model. Moreover, the

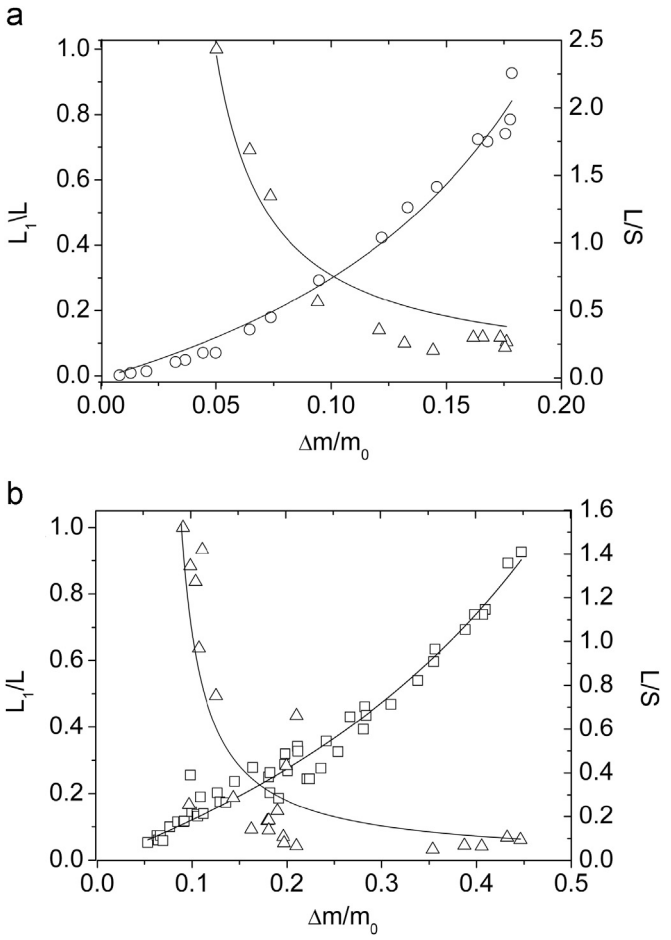

Fig. 12. a. The tightly bound water in units of total liquid signal, L_1 /L, (open triangles) and the total liquid signal in units of solid, L/S, (open circles) hydration dependence for horse chestnut (*Aesculus hippocastanum* L.) bast. The solid lines were calculated from Eq. (6) and from Eq. (11), respectively. b. The tightly bound water in units of total liquid signal, L_1 /L, (open triangles) and the total liquid signal in units of solid, L/S, (open circles) hydration dependence for *Usnea antarctica*. The solid lines were calculated from Eq. (6) and from Eq. (11), respectively.

increase in the levels of monosaccharides (releasing from glucans) and polyols (as a product of following algal and fungal cells metabolism) can support osmotic potential of cells leading to further water uptake [48].

In horse chestnut *Aesculus hippocastantum* most of water-soluble solid fraction consists mainly of sucrose. The dissolution process occurs without enzymatic action. The hydration level at which the total portion of the water-soluble solid fraction totally dissolves is directly observed in horse chestnut bast. It equals $\Delta M/m_0=0.180$, which responds for the total amount of water-soluble solid fraction equal to $\Delta M_c/m_0=0.325$. Also the NMR signal from tightly bound water fraction, L_1, is detected in wide range of hydration [3].

Thus, we recalculated the data for horse chestnut bast and fitted Eq. (6) to the hydration dependency of L_1/L, and Eq. (11) to the hydration dependence of L/S (see Fig. 12(a)). The combined fit of these two Equations yields $c_s=(74.5\pm5.1)\%$, which is a little higher than 64.3% obtained using more precise model applied by them [3], and higher than those for sucrose ($c_s=68\%$). For this fitting we used $\gamma=0.59$, which is the averaged value for biological carbohydrates, as the polyol fraction for horse chestnut bast is negligible. The difference in fitted values between our and their model is a measure of real accuracy of our model. However, it may be applied in case the limit of total water-soluble solid fraction dissolution is beyond the measured hydration level range or if it does not exist at all as it is in case of germinating seeds.

In addition, we recalculated (for $\gamma=0.63\pm0.08$) some already published data for other species of fruticose lichenized fungi, *eg.* for *Usnea antarctica* [6]. The combined fit to Eq. (6) and to Eq. (11), respectively, yields $c_s=0.81\pm0.04$, which is close to the value obtained by us for *Cetraria aculeata* (Fig. 12b). This suggests a similar way of recovery of the lichen metabolism from cryptobiotic form at dehydration, *i.e.* by the solid carbohydrate and polyol dissolution.

6. Conclusions

The hydration dependency of high power ^{1}H NMR spectra for a dehydrated thallus of *Cetraria aculeata* shows two fractions of residual bound water which differ in mobility, *i.e.* tightly and loosely bound water, and the presence of the water soluble solid fraction in the thallus. The proposed simple model allows the quantitative description of that effect and yields the saturation concentration of the discovered water soluble solid fraction. The applicability of proposed model may also extend to other tissues/organisms at drastically low hydration level, as *e.g.* horse chestnut bast, other species of lichenized fungi or germinating seeds.

Acknowledgements

The research was carried out with the equipment purchased thanks to the financial support of the European Regional Development Fund in the framework of the Polish Innovation Economy Operational Program (contract no. POIG.02.01.00-12-023/08) and also financed by the Polish Ministry of Science and Higher Education (MNiSW, contract no. 7150/E-338/M/2015).

Appendix A. Transparency document

Transparency document associated with this article can be found in the online version at doi:10.1016/j.bbrep.2016.04.010.

References

[1] H. Harańczyk, A. Leja, K. Strzałka, The effect of water accessible paramagnetic ions on subcellular structures formed in developing wheat photosynthetic membranes as observed by NMR and by sorption isotherm, Acta Phys. Pol. A109 (2006) 389–398.
[2] H. Harańczyk, A. Leja, M. Jemioła-Rzemińska, K. Strzałka, Maturation processes of photosynthetic membranes observed by proton magnetic relaxation and sorption isotherm, Acta Phys. Pol. A115 (2009) 526–532.
[3] H. Harańczyk, W.P. Węglarz, Z. Sojka, The investigation of hydration processes in horse chestnut (*Aesculus hippocastanum*, L.) and pine (*Pinus silvestris*, L.) bark and bast using proton magnetic relaxation, Holzforschung 53 (1999) 299–310.
[4] H. Harańczyk, K. Strzałka, G. Jasiński, K. Mosna-Bojarska, The initial stages of wheat (*Triticum aestivum*, L.) seed imbibition as observed by proton nuclear magnetic relaxation, Colloids Surf. A115 (1996) 47–54.
[5] H. Harańczyk, On water in extremely dry biological systems, WUJ, Kraków, 2003.
[6] H. Harańczyk, Ł. Pater, P. Nowak, M. Bacior, M.A. Olech, Initial phases of Antarctic *Ramalina terebrata* Hook f. & Taylor thalli rehydration observed by proton relaxometry, Acta Phys. Pol. A 121 (2012) 478–482 2012.
[7] H. Harańczyk, M. Bacior, M.A. Olech, Deep dehydration of *Umbilicaria aprina* thalli observed by proton NMR and sorption isotherm, Antarct. Sci. 20 (2008) 527–535.
[8] H. Harańczyk, M. Bacior, P. Jastrzębska, M.A. Olech, Deep dehydration of Antarctic lichen *Leptogium puberulum* Hue observed by NMR and sorption isotherm, Acta Phys. Pol. A115 (2009) 516–520.
[9] H. Harańczyk, P. Nowak, M. Bacior, M. Lisowska, M. Marzec, M. Florek, M. A. Olech, Bound water freezing in *Umbilicaria aprina* from continental Antarctica, Antarct. Sci. 24 (2012) 342–352.
[10] M. Barták, P. Váczi, Josef Hájek, J. Smykla, Low-temperature limitation of

primary photosynthetic processes in Antarctic lichens *Umbilicaria antarctica* and *Xanthoria elegans*, Polar Biol. 31 (2007) 47–51.
[11] H.E. Hinton, A new chironomid from Africa, the larva of which can be dehydrated without injury, Proc. Zool. Soc. Lond. 121 (1951) 371–380.
[12] H.E. Hinton, Cryptobiosis in the larva of *Polypedilum vanderplanki* Hint. (Chironomidae), J. Insect Physiol. 5 (1960) 286–300.
[13] M. Watanabe, T. Kikawada, N. Minagawa, F. Yukuhiro, T. Okuda, Mechanism allowing an insect to survive complete dehydration and extreme temperatures, J. Exp. Biol. 205 (2002) 2799–2802.
[14] M. Watanabe, T. Kikawada, T. Okuda, Increase of internal ion concentration triggers trehalose synthesis associated with cryptobiosis in larvae of *Polypedilum vanderplanki*, J. Exp. Biol. 206 (2003) 2281–2286.
[15] M. Sakurai, T. Furuki, Ken.-ichi. Akao, D. Tanaka, Y. Nakahara, T. Kikawada, Vitrification is essential for anhydrobiosis in an African chironomid, *Polypedilum vanderplanki*, Proc. Natl. Acad. Sci. USA 105 (2008) 5093–5098.
[16] T. Shimizu, Y. Kanamori, T. Furuki, T. Kikawada, T. Okuda, T. Takahashi, H. Mihara, M. Sakurai, Desiccation-induced structuralization and glass formation of group 3 late embryogenesis abundant protein model peptides, Biochemistry 49 (2010) 1093–1104.
[17] T.W. Hegarty, The physiology of seed hydration and dehydration, and the relation between water stress and the control of germination: a review, Plant Cell Environ. 1 (1978) 101–119.
[18] W.M. Lush, R.H. Groves, Germination, emergence and surface establishment of wheat and ryegrass in response to natural and artificial hydration-dehydration cycles, Aust. J. Agric. Res. 32 (1981) 731–739.
[19] J.D. Bewley, M. Black, Physiology and Biochemistry of Seeds in Relation to Germination, Springer-Verlag, Berlin, Heidelberg, 1978.
[20] N. Hamada, K. Okazaki, M. Shinozaki, Accumulation of monosaccharides in lichen mycobionts cultured under osmotic conditions, Bryologist 97 (1994) 176–179.
[21] D.R. Melick, R.D. Seppelt, The effect of hydration on carbohydrate levels, pigment content and freezing point of *Umbilicaria decussata* at a continental Antarctic locality, Cryptogam. Bot. 4 (1994) 212–217.
[22] J. Hájek, P. Váczi, M. Barták, Photosynthetic electron transport at low temperatures in the green algal foliose lichens *Lasalia pustulata* and *Umbilicaria hirsuta* affected by manipulated levels of ribitol, Photosynthetica 47 (2009) 199–205.
[23] H. Harańczyk, M. Bacior, J. Jamróz, M. Jemioła-Rzemińska, K. Strzałka, Rehydration of DGDG (digalactosyl diacylglicerol) model membrane lyophilizates observed by NMR and sorption isotherm, Acta Phys. Pol. A115 (2009) 521–525.
[24] M. Witek, W.P. Węglarz, L. de Jong, G. van Dalen, J.C.G. Blonk, P. Heussen, E. Van Velzen, H. Van As, J. van Duynhoven, The structural and hydration properties of heat-treated rice studied at multiple length scales, Food Chem. 120 (2010) 1031–1040.
[25] R. Khanna, S. Rajan, Govindjee, H.S. Gutowsky, Effects of physical and chemical treatments on chloroplast manganese. NMR and ESR studies, Biochim. Biophys. Acta 725 (1983) 10–18.
[26] N.S. Murthy, C.R. Worthington, X-ray diffraction evidence for the presence of discrete water layers on the surface of membranes, Biochim. Biophys. Acta 1062 (1991) 172–176.
[27] W.C. de Baat, Sur l'acide dithionique et ses sels, Recl. Trav. Chim. Pays-Bas 45 (1926) 237–244.
[28] W.M. Meylan, P.H. Howard, R.S. Boethling, Improved method for estimating water solubility from octanol/water partition coefficient, Environ. Toxicol. Chem. 15 (1996) 100–106.
[29] The Merck index: an encyclopedia of chemicals, drugs, and biological, Rahway, N.J., U.S.A.: Merck, New York (1996, 2006).
[30] J.W. Mullin, Crystallisation, Butterworth, London 1972, p. 425.
[31] S.H. Yalkowsky and R.M. Dannenfelser. Aquasol Database of Aqueous Solubility, Version 5, College of Pharmacy, Univ. of Ariz, Tucson, AZ. PC Version, 1992.
[32] T. Higashiyama, Novel functions and applications of trehalose, Pure Appl. Chem. 74 (2002) 1263–1269.
[33] L.B. Lahuta, W. Święcicki, T. Dzik, R.J. Górecki, M. Horbowicz, Feeding stem-leaf-pod explants of pea (*Pisum sativum* L.) with d-*chiro*-inositol or d-pinitol modifies composition of α-D-galactosides in developing seeds, Seed Sci. Res. 20 (2010) 213–221.
[34] D.F. Gaff, Desiccation tolerant vascular plants of Southern Africa, Oecologia 31 (1977) 95–109.
[35] W.P. Węglarz, H. Harańczyk, Two-dimensional analysis of the nuclear relaxation function in the time domain: the program CracSpin, J. Phys. D Phys 33 (2000) 1909–1920.
[36] S. Brunauer, P.H. Emmett, E. Teller, Adsorption of gases in multimolecular layers, J. Am. Chem. Soc. 60 (1938) 309–319.
[37] R.W. Dent, A multilayer theory for gas sorption. Part I: Sorption of a single gas, Text. Res. J. 47 (1977) 145–152.
[38] W.P. Weglarz, H. Peemoeller, A. Rudin, Characterization of annealed isotactic polypropylene in the solid state by 2D time-domain ^{1}H NMR, J. Polym. Sci. B: Polym. Phys. 38 (2000) 2487–2506.
[39] W. Derbyshire, M. Van Den Bosch, D. Van Dusschoten, W. MacNaughtan, I. A. Farhat, M.A. Hemminga, J.R. Mitchell, Fitting of the beat pattern observed in NMR free-induction decay signals of concentrated carbohydrate-water solutions, J. Magn. Res 168 (2004) 278–283.
[40] A.A. Abragam, The Principles of Nuclear Magnetism, Clarendon Press,, Oxford, 1961.
[41] H. Harańczyk, J. Czak, P. Nowak, J. Nizioł, Initial phases of DNA rehydration by NMR and sorption isotherm, Acta Phys. Pol. A117 (2010) 257–262.
[42] M.M. Pintar, Some considerations of the round table subject, Magn. Reson. Imaging 9 (1991) 753–754.
[43] A. Timur, Pulsed nuclear magnetic resonance studies of porosity, movable fluid, and permeability of sandstones, J. Pet. Technol. 21 (1969) 775–786.
[44] R. Honegger, A. Haisch, Immunocytochemical location of the (1→3) (1→4)-β-glucan lichenin in the lichen-forming ascomycete *Cetraria islandica* (Icelandic moss), New Phytol. 150 (2001) 739–746.
[45] A. Lazaridou, C.G. Biliaderis, Molecular aspects of cereal β-glucan functionality: Physical properties, technological applications and physiological effects, J. Cereal Sci. 46 (2007) 101–118.
[46] R.A. Burton, G.B. Fincher, (1,3;1,4)-β-D-Glucans in cell walls of the Poaceae, lower plants, and fungi: a tale of two linkages, Mol. Plant 2 (2009) 873–882.
[47] A.M. Corder, R.J. Henry, Carbohydrate-degrading enzymes in germinating wheat, Cereal Chem. 66 (1989) 435–439.
[48] L. Gustavs, A. Eggert, D. Michalik, U. Karsten, Physiological and biochemical responses of green microalgae from different habitats to osmotic and matric stress, Protoplasma 243 (2010) 3–14.